Macromolecular Rapid Communications
www.mrc-journal.de

Flaw-Insensitive Hydrogels under Static and Cyclic Loads

*Ruobing Bai, Jiawei Yang, Xavier P. Morelle, and Zhigang Suo**

New applications of hydrogels draw growing attention to the development of tough hydrogels. Most tough hydrogels are designed through incorporating large energy dissipation from breaking sacrificial bonds. However, these hydrogels still fracture under prolonged cyclic loads with the presence of even small flaws. This paper presents a principle of flaw-insensitive hydrogels under both static and cyclic loads. The design aligns the polymer chains in a hydrogel at the molecular level to deflect a crack. To demonstrate this principle, a hydrogel of polyacrylamide and polyvinyl alcohol is prepared with aligned crystalline domains. When the hydrogel is stretched in the direction of alignment, an initial flaw deflects, propagates along the loading direction, peels off the material, and leaves the hydrogel flawless again. The hydrogel is insensitive to pre-existing flaws, even under more than ten thousand loading cycles. The critical degree of anisotropy to achieve crack deflection is quantified by experiments and fracture mechanics. The principle can be generalized to other hydrogel systems.

Hydrogel-based soft devices have been extensively developed in recent years. Examples include soft robots,[1,2] skin-like sensors,[3–7] stretchable optical fibers,[8] transparent triboelectric generators,[9] and stretchable ionotronic devices.[10–14] The working conditions of these applications involve prolonged, repeated mechanical loads, thus require hydrogels to maintain their functionalities, as well as their mechanical robustness and stretchability over a long time. However, all hydrogels are susceptible to fracture due to the existence of flaws such as cavities, cracks, and impurities, to different degrees.[15–17] The sensitivity to flaw of a soft, elastic hydrogel can be estimated by a critical length scale Γ/W_c, where Γ is the fracture toughness, and W_c is the work to rupture measured with no or negligible flaw.[15] A hydrogel is not sensitive to a pre-existing flaw with size smaller than Γ/W_c. Tough hydrogels have been developed with Γ over thousands of J m^{-2}, and have significantly enhanced this flaw-sensitivity length.[18–27] For example, a tough double-network hydrogel, if assumed as an elastic-plastic material during its first-time loading, has $\Gamma \approx 10^4$ J m^{-2} and $W_c \approx 10^5$ J m^{-3}, leading to a critical flaw-sensitivity length scale of $\Gamma/W_c \approx 0.1$ m. In comparison, a single-network hydrogel, such as polyacrylamide, has $\Gamma \approx 10^2$ J m^{-2}, $W_c \approx 10^5$ J m^{-3}, and $\Gamma/W_c \approx 10^{-3}$ m.

Despite this enhancement of toughness, one significant issue remains. All the tough hydrogels reported so far rely on the large energy dissipation from breaking the sacrificial bonds in the hydrogels. The energy dissipation is large when the hydrogel is loaded for the first time, but is often poorly reversible in the subsequent loading cycles, due to the irreversible nature of the bonds (e.g., covalent bonds), or the relatively short time allowed for recovery of the bonds (e.g., most mechanical motions work with periods shorter than a few minutes). Ultimately, all hydrogels suffer fatigue fracture, that is, the gradual extension of crack from an initial flaw under cyclic loads.[28–33] The highest threshold for fatigue fracture of a double-network, tough hydrogel reported up-to-date is about 400 J m^{-2}, still only 1/10 of its bulk fracture toughness.[32]

Life has found another way to be tough. Shells,[34] skins,[35] bones,[36,37] and cartilage[38] are flaw-insensitive by a microstructural design. In all the above examples, the microstructures generate mechanical anisotropy, which leads to crack deflection. Such crack deflection shields the zone that needs protection in the biological materials. One example is the toughening of human bones. Under loading, the osteons and their brittle interfaces can divert the crack path from the plane of maximum stress of an initial flaw, and reduce the stress intensity at the crack tip.[36,37] Designing crack deflection has been applied in many materials including metals, ceramics, elastomers, and composites,[39,40] but has not been explored in hydrogels. In particular, most current designs for crack deflection rely on composites, with directional fibers or aligned inclusions.

Here we describe a principle of flaw-insensitive hydrogels under both static and cyclic loads through crack deflection. We achieve crack deflection in hydrogels through the alignment of polymer chains at the molecular level. The aligned polymer chains induce anisotropy, making the hydrogel mechanically weaker between the chains due to the non-covalent inter-chain bonding, but stronger along the chains due to the covalent intra-chain bonding. When such a hydrogel is loaded along the aligned direction, a pre-existing flaw deflects from its initial direction of propagation, runs along the loading direction, peels off the material, and protects the remaining hydrogel.

To demonstrate this principle, we synthesized a hybrid hydrogel of polyvinyl alcohol (PVA) and polyacrylamide (PAAm).

Dr. R. Bai, Dr. J. Yang, Dr. X. P. Morelle, Prof. Z. Suo
John A. Paulson School of Engineering and Applied Sciences
Harvard University
Cambridge, MA 02138, USA
E-mail: suo@seas.harvard.edu
Dr. R. Bai, Dr. J. Yang, Dr. X. P. Morelle, Prof. Z. Suo
Kavli Institute for Bionano Science and Technology
Harvard University
Cambridge, MA 02138, USA
The ORCID identification number(s) for the author(s) of this article can be found under https://doi.org/10.1002/marc.201800883.

DOI: 10.1002/marc.201800883

The PVA network forms aligned crystals through mechanical stretching, and the PAAm network provides elasticity and supports the stretching. We crystallized the PAAm-PVA hydrogel through a one-step soaking method (**Figure 1a**). Other methods to form crystalline PVA hydrogels include freeze-thaw[41–44] and cast-dry.[22,45,46] Both methods require large change of either temperature or water content of the hydrogel, and usually take several processing cycles for sufficient crystallization. Adding

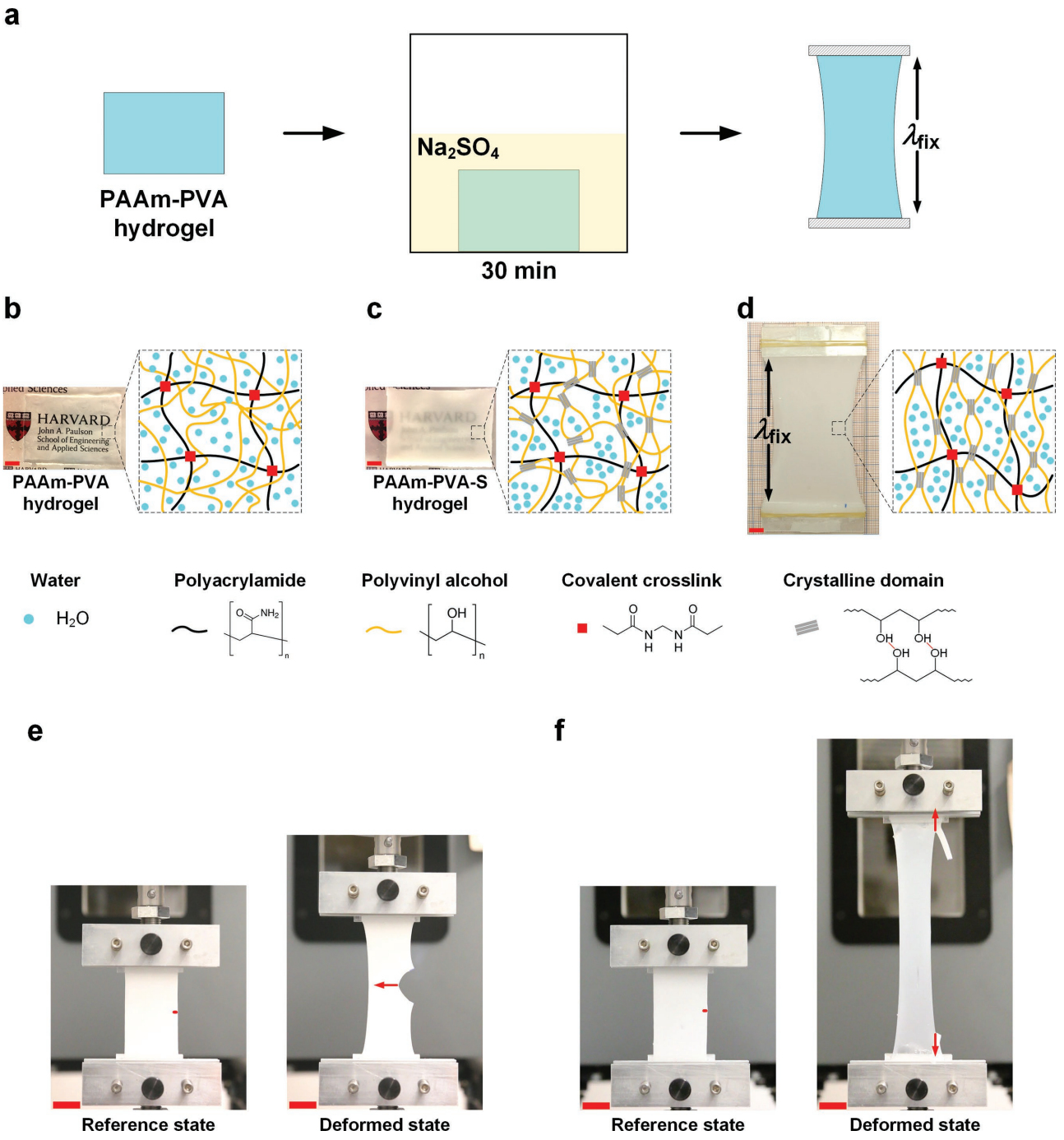

Figure 1. Preparation of the flaw-insensitive PAAm-PVA-S hydrogel with aligned PVA crystalline domains. a) The PAAm-PVA hydrogel is soaked in Na_2SO_4 solution for 30 min, and then mechanically stretched to a prescribed stretch λ_{fix}. b) The initial PAAm-PVA hydrogel has no crystalline domains and appears transparent. c) After soaking, the resulting PAAm-PVA-S hydrogel forms crystallization and becomes translucent. d) The PAAm-PVA-S hydrogel is subsequently stretched and the PVA chains form aligned crystallization. The scale bar in (b)–(d) is 1 cm. e) An initial flaw (≈3 mm) in an unaligned PAAm-PVA-S hydrogel quickly propagates throughout the sample once the hydrogel is stretched (Movie S1, Supporting Information). f) The same-size initial flaw in an aligned hydrogel does not propagate across the sample, but deflects along the loading direction and peels off the material piece containing the flaw, leaving the hydrogel flawless again (Movie S2, Supporting Information). The scale bar in (e) and (f) is 2 cm.

specific salt such as Na_2SO_4 into the PVA solution can enhance the crystallization.[44,45] The kosmotropic sulfate ions enhance the stability of the interaction between water molecules, and therefore reduce the number of water molecules interacting with the PVA chains, increasing the hydrogen bonding between the PVA chains. In the current method, we first made a covalently crosslinked PAAm hydrogel with uncrosslinked PVA chains (PAAm-PVA hydrogel). The hydrogel has no crystalline domains of PVA, and is highly transparent (Figure 1b). We then soaked the PAAm-PVA hydrogel into Na_2SO_4 solution of 0.6 M for 30 min. The resulting hydrogel (PAAm-PVA-S) became translucent (Figure 1c), indicating the crystallization of PVA. The PAAm-PVA-S hydrogel prepared in this way has the similar stress–stretch response compared to that prepared by the traditional freeze-thaw method (Figure S1, Supporting Information). In addition, good self-recovery of the stress–stretch curve was found within 1 h after the hydrogel was loaded for the first time (Figure S2, Supporting Information). To align the PVA chains, we fixed the hydrogel into a customized acrylic mold with a prescribed stretch λ_{fix}. The pre-stretch λ_{fix} is tunable, and allows further alignment and crystallization growth of the PVA chains along the stretching direction in a controlled manner (Figure 1d).

We test the flaw sensitivity of both the unaligned and the aligned PAAm-PVA-S hydrogels by cutting an initial flaw of ≈3 mm on the edge of each sample, and uniaxially stretching the sample. For the unaligned hydrogel, the flaw quickly fractured through the entire sample once the hydrogel started being stretched (Figure 1e & Movie S1, Supporting Information). In contrast, the flaw in the aligned hydrogel with $\lambda_{fix} = 2.5$ simply peeled off the small material piece containing it along the loading direction, leaving the sample flawless again. No fracture occurred in the remaining hydrogel until the end of test (Figure 1f & Movie S2, Supporting Information).

The additional aligned crystallization growth of PVA in the hydrogel after soaking benefits from its slow crystallization kinetics induced by Na_2SO_4. Without a soaking in Na_2SO_4 or any mechanical stretch λ_{fix}, the stress–stretch curve of the PAAm-PVA hydrogel keeps the same for 7 days after the polymerization (**Figure 2a**), indicating no growth of crystallization. By contrast, the stress–stretch curve of an unstretched PAAm-PVA-S hydrogel after soaking keeps stiffening daily, until reaching saturation after 7 days (Figure 2b). The soaked hydrogel becomes much stiffer than the unsoaked one even from the first day of measurement. The daily stiffening of the stress–stretch curve indicates the gradual growth of crystallization. The prescribed stretch λ_{fix} then further guides such gradual crystallization growth, and builds up mechanical anisotropy in the PAAm-PVA-S hydrogel. The PAAm-PVA-S hydrogel with $\lambda_{fix} = 2.5$ for 5 days shows clear anisotropy in stress–stretch curves in the aligned and transverse directions (Figure 2c). Similar effect of mechanical anisotropy can be achieved through other stretching profiles (Figures S3 and S4, Supporting Information). To verify the crystalline structures microscopically, we linked the fluorescent dye 5-DTAF to the hydroxide groups on PVA (see Figure S5, Supporting Information, for the chemical

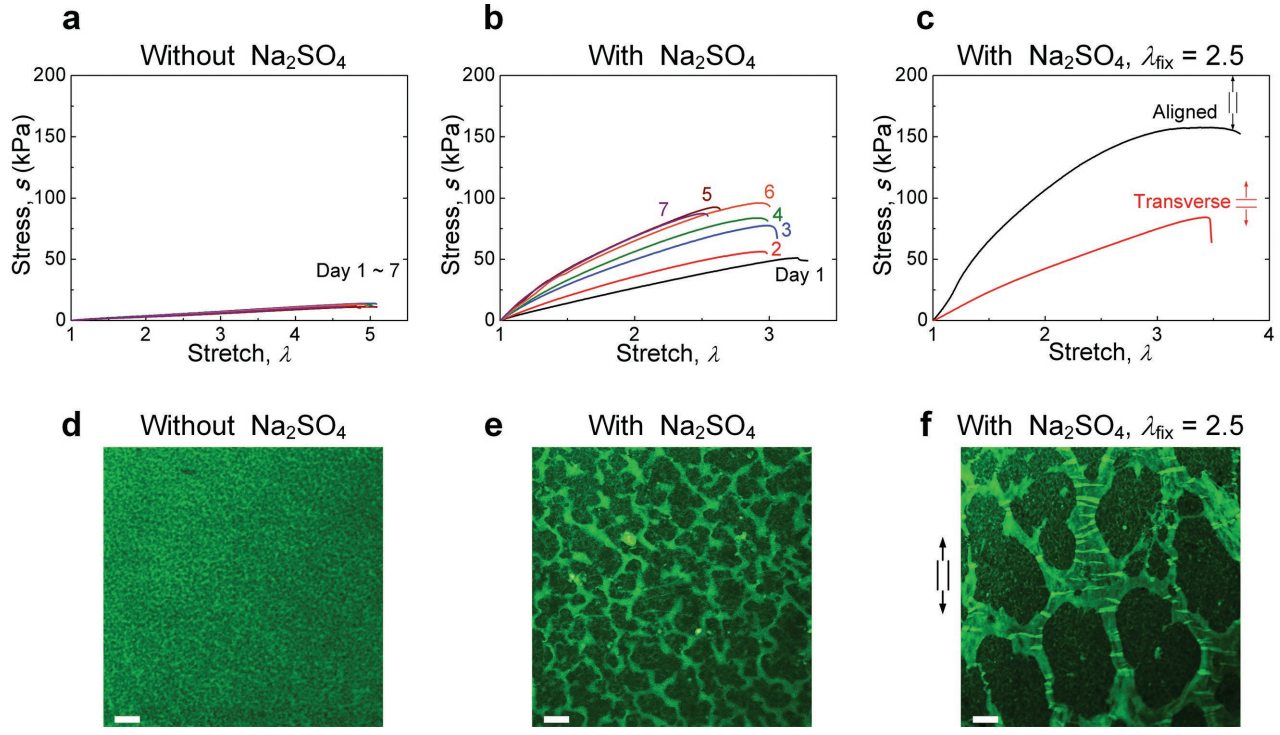

Figure 2. Kinetics of the Na_2SO_4-induced PVA crystallization. a) Without Na_2SO_4, no crystallization forms in the PAAm-PVA hydrogel over 7 days. The stress–stretch curve remains the same every day. b) With Na_2SO_4, the crystallization grows gradually in the PAAm-PVA-S hydrogel, and stiffens the stress–stretch curve every day. c) The directional crystallization in an aligned PAAm-PVA-S hydrogel with $\lambda_{fix} = 2.5$ leads to anisotropic stress–stretch behaviors. The confocal images (d), (e), and (f) exhibit the microscopic structures of the above three corresponding hydrogels. Each curve in (a)–(c) represents 3–5 experimental results. The scale bar in (d)–(f) is 20 μm.

reaction). The PVA-rich regions in the resulting hydrogels show a brighter color under confocal microscopy. The PAAm-PVA hydrogel without soaking shows a homogeneous distribution of PVA (Figure 2d), indicating no formation of crystallization. The unaligned PAAm-PVA-S hydrogel shows homogeneous, brighter PVA-rich crystalline domains surrounded by darker PVA-poor regions, with no preferred direction of the domain distribution (Figure 2e). The aligned PAAm-PVA-S hydrogel shows directional, coarsened crystalline domains, proving the effect of mechanical stretching (Figure 2f). The effect of mechanical stress on anisotropic coarsening has been studied in many materials.[47,48] Here the coarsening is possibly due to the enhanced crystallization of PVA chains under the mechanical alignment.

The degree of anisotropy in the PAAm-PVA-S hydrogel is tunable by the pre-stretch λ_{fix}. For all the hydrogels with different values of λ_{fix}, we observed stiffening of the stress–stretch curve in the aligned direction (**Figure 3a**), and softening in the transverse direction (Figure 3b). The elastic modulus increases with λ_{fix} in the aligned direction, and decreases in the transverse direction (Figure 3c). We measured the fracture toughness of the hydrogels in both directions under different λ_{fix}. The chain alignment toughens the hydrogel in the aligned direction, and embrittles the hydrogel in the transverse direction (Figure 3d). Crack deflection starts to be observed in hydrogels from $\lambda_{fix} > 1.2$.

We characterize the critical condition for crack deflection by comparing the fracture toughness in the two directions. We define the fracture toughness in the direction along the crack tip as Γ_1, and the fracture toughness perpendicular to the crack tip as Γ_2 (inset of Figure 3e). The dimensionless parameter, $\alpha = \Gamma_2/\Gamma_1$, quantifies the degree of anisotropy in terms of the fracture toughness. When $\lambda_{fix} = 1.0$ and $\alpha = 1.0$, the material is isotropic, and the crack will propagate along its initial direction under uniaxial loading. As λ_{fix} increases, the material becomes more brittle in the direction of Γ_2, and tougher in the direction of Γ_1, and α becomes smaller. When α further decreases to reach a critical value of α_{cr}, the material becomes too brittle in the perpendicular direction, and the crack starts deflecting.

The theoretical value of α_{cr} calculated from the fracture mechanics of a linear, isotropic elastic material is 0.26.[49,50] For the current hydrogel under large deformation, we determine an upper bound of α_{cr} experimentally as following. We plot $\alpha = \Gamma_2/\Gamma_1$ as a function of λ_{fix} (Figure 3e), together with the path of crack propagation in each case (see Figure S6 and Movies S3 – S6, Supporting Information, for the complete propagation). $\lambda_{fix} = 1.0$ corresponds to an isotropic hydrogel, and the crack propagates along its initial direction under loading. When $\lambda_{fix} = 1.1$, we calculate through measurement that $\alpha = 0.8$. The transverse direction becomes brittle, but not enough for crack deflection. When $\lambda_{fix} = 1.2$ and $\alpha = 0.3$, the transverse direction becomes further brittle, and the crack kinks to approximately 45°. Following the propagation, the crack goes up and down through a serpentine path. When $\lambda_{fix} = 1.3$, the crack deflects, and Γ_1 cannot be experimentally measured any more. The critical condition for crack deflection in the current hydrogel is thus $\alpha_{cr} < 0.3$, close to the theoretical value of $\alpha = 0.26$ predicted by linear elastic fracture mechanics.

The anisotropic PAAm-PVA-S hydrogel is insensitive to pre-existing flaws under cyclic loads. To demonstrate, we prepared two hydrogel samples with identical composition but $\lambda_{fix} = 1.0$ and $\lambda_{fix} = 2.5$, respectively. We notched both samples with an initial flaw of 3 mm on the edge. We then cyclically loaded the samples with a peak stretch $\lambda_{max} = 2.2$ (**Figure 4a**). Neither sample fractured after the first loading cycle. However, the small flaw quickly evolved and propagated through the entire sample with $\lambda_{fix} = 1.0$ in 100 cycles (Figure 4b). In comparison, the flawed sample with $\lambda_{fix} = 2.5$ sustained more than 10 000 cycles without any crack propagation along the horizontal direction (Figure 4c). Instead, a slight crack deflection took place in the vertical direction and reduced the stress concentration at the crack tip. The anisotropic hydrogel is insensitive to pre-existing flaws under cyclic loads, without requiring additional energy dissipation mechanism.

The more complete fatigue fracture characterization of these hydrogels was conducted using long initial cracks (20 mm). For the PAAm-PVA-S hydrogel with $\lambda_{fix} = 2.5$, the threshold for fatigue fracture in the transverse direction is 44.0 J m^{-2} (Figure S7, Supporting Information), comparable to the threshold measured in other hydrogels with a PAAm network.[29–33] In the aligned direction, crack deflection was observed to extend vertically to the ends of the sample (Figure S8, Supporting Information). For the isotropic PAAm-PVA-S hydrogel with $\lambda_{fix} = 1.0$, crack deflection also can appear when the hydrogel was loaded under large λ_{max} for many cycles (Figure S9, Supporting Information). We hypothesize that the PVA chains tend to align under cyclic large stretch and prompt the directional crystallization. This dynamic, spontaneous alignment deflects the crack and enhances the resistance to fatigue fracture even for an initially isotropic hydrogel.

The incapability of enhancing the fatigue fracture resistance of hydrogels by incorporating large energy dissipation lies in the nature of polymer chain fracture at the crack tip. In general, toughening a material can result from two parts: the intrinsic toughening and the extrinsic toughening. The intrinsic toughening depends on the local fracture zone ahead of the crack tip, and the extrinsic toughening depends on mechanisms behind the crack tip, such as the large area of energy dissipation and crack deflection.[23,25,51,52] For a tough hydrogel incorporating large energy dissipation, the intrinsic toughness Γ_{in} depends on the local polymer chain fracture at the crack tip, while the extrinsic toughness Γ_{ex} depends on the energy dissipation.[23,25] Γ_{ex} can be easily enhanced over thousands of J m^{-2} through breaking a large amount of weak bonds behind the crack tip, while Γ_{in} is mostly on the order of 10–100 J m^{-2}, limited by the nature of hydrogel network.[23,25,28–33] At last, the threshold for fatigue fracture only depends on the intrinsic toughness Γ_{in}, but negligibly on Γ_{ex}.[28,31,33,51]

Aligning polymer chains to toughen a soft material has been successfully applied in many commercial products such as ultra-stiff, tough, and fatigue-resistant fibers including isotactic polypropylene[53] and polyethylene.[54] In addition, a natural rubber is isotropic in the undeformed state, but becomes anisotropic due to the aligned inter-chain crystallization when subject to a stretch. Such stretch-induced crystallization also enables crack deflection and helps the natural rubber sustain cyclic loads.[55,56] Introducing crack deflection for fracture resistance,

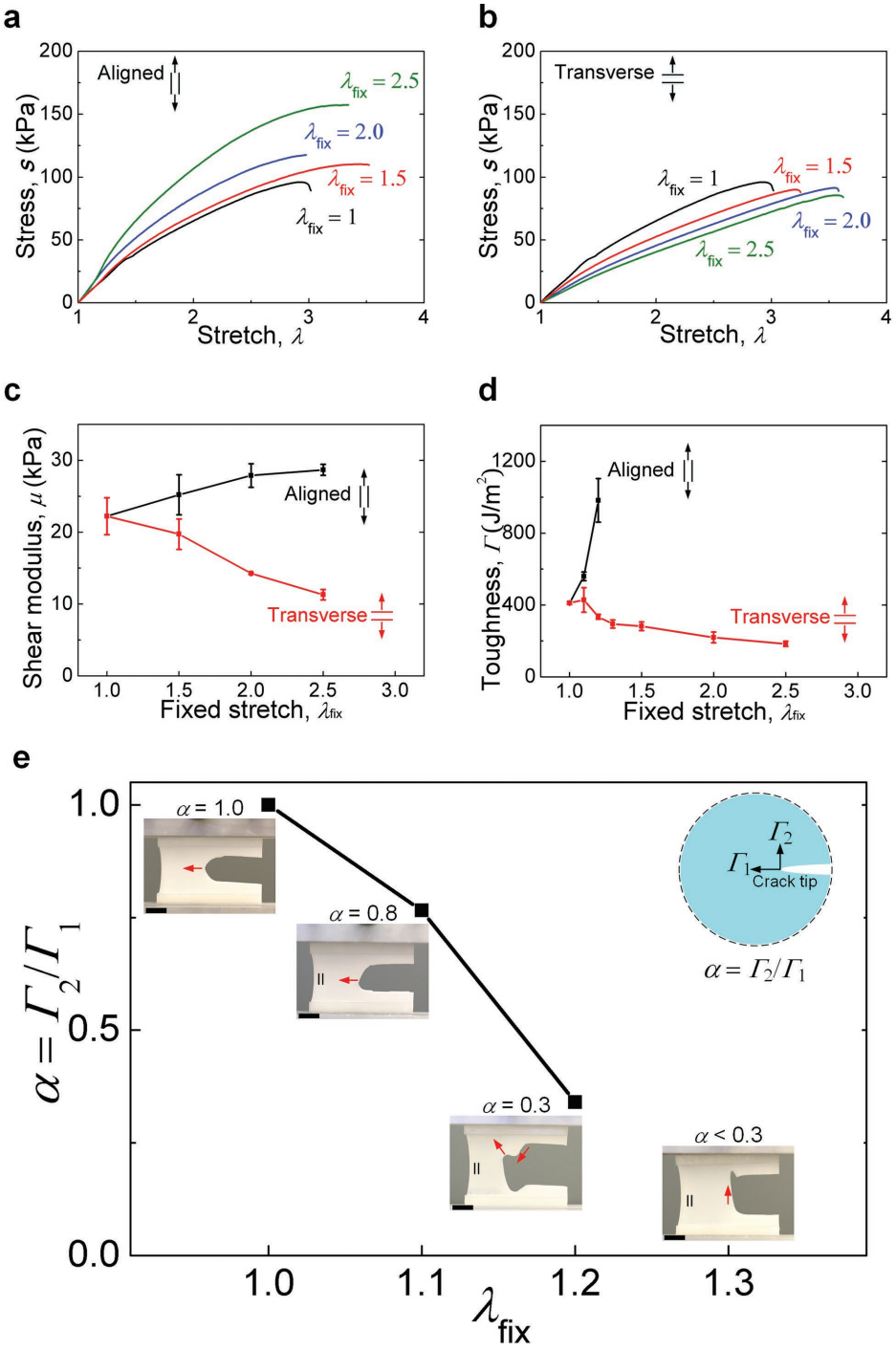

Figure 3. The analysis of the tunable degree of anisotropy prescribed by λ_{fix}, and its effect on the crack deflection. The stress–stretch curves show that with increasing λ_{fix}, the hydrogel becomes a) stiffer in the aligned direction and b) more compliant in the transverse direction. c) The corresponding shear modulus changes with λ_{fix}. d) With increasing λ_{fix}, the hydrogel becomes tougher in the aligned direction, but more brittle in the transverse direction. e) The degree of anisotropy in terms of the fracture toughness is represented by $\alpha = \Gamma_2/\Gamma_1$. α decreases with λ_{fix}, and reaches $\alpha < 0.3$ when crack deflection occurs at $\lambda_{fix} = 1.3$. The inset photos show the crack path in hydrogels with $\lambda_{fix} = 1.0$, 1.1, 1.2, and 1.3. Also see Figure S6, Supporting Information, and Movies S3–S6, Supporting Information, for the complete crack path. Each curve in (a) and (b) represents 3–5 experimental results. Each data point in (c) and (d) represents the mean and standard deviation of 3–5 experimental results. The scale bar in (e) is 1 cm.

especially under cyclic loads, can be further generalized to many hydrogel systems. Most current tough hydrogels contain two or more polymer networks, with one providing elasticity, and the other one dissipating energy. One can readily align one of the polymer networks in such a tough hydrogel and form anisotropy. Methods have already been developed to align the

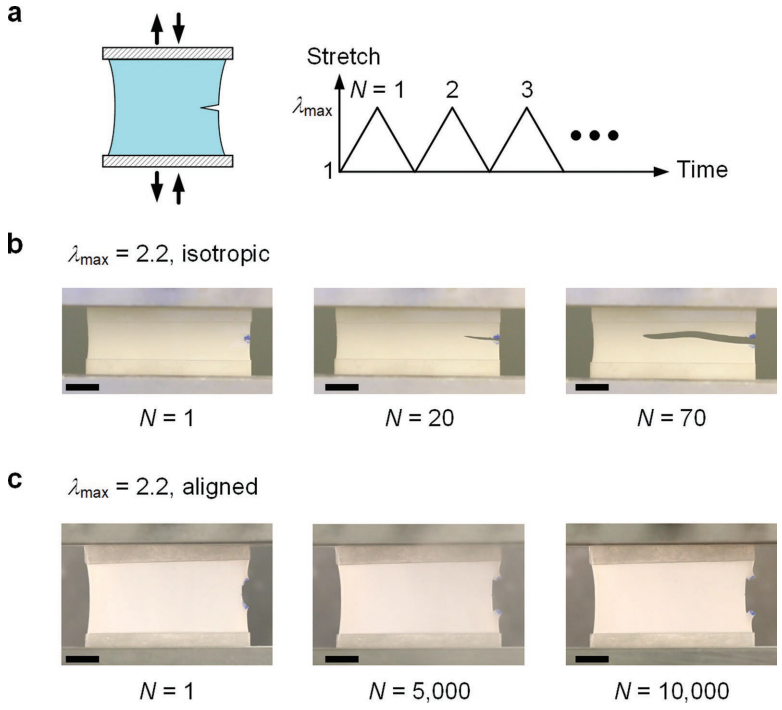

Figure 4. Flaw-insensitivity under cyclic loads. a) A hydrogel is notched with an initial flaw (≈3 mm) and cyclically stretched. b) An unaligned PAAm-PVA-S hydrogel with the initial flaw completely fractures within 100 loading cycles. c) An aligned hydrogel with $\lambda_{fix} = 2.5$ sustains over 10 000 loading cycles. The scale bar is 1 cm.

polymer chains in hydrogels, such as microfluidics,[57] shear flow,[21] and mechanical stretching.[58–60] Finally, a hydrogel resisting cracks in all directions can be achieved by laminating the anisotropic sheets.

In summary, we have described a principle of flaw-insensitive hydrogels under both static and cyclic loads through crack deflection. We demonstrate this principle through a hydrogel of polyacrylamide and polyvinyl alcohol. Under stretching, an initial flaw in the hydrogel deflects and peels off the small piece of material, leaving the hydrogel flawless again. The critical degree of anisotropy for crack deflection is close to the theoretical prediction from linear elastic fracture mechanics. The anisotropic hydrogel can sustain more than ten thousand loading cycles without failure. The current design is readily generalized to other hydrogel systems, which can benefit future applications that require hydrogels to sustain prolonged cyclic loads.

Experimental Section

Preparation of materials: The following substances were purchased from Sigma Aldrich: acrylamide (AAm, A8887), *N,N′*-methylenebis(acrylamide) (MBAA, M7279), *N,N,N′,N′*-tetramethylethylenediamine (TEMED, T7024), ammonium persulfate (APS, A9164), polyvinyl alcohol (PVA, 341584) and sodium sulfate (Na_2SO_4, anhydrous, 1614807). All chemicals were received and used without further purification.

The PAAm-PVA hydrogel was synthesized in the following way. PVA powder (M_w 89 000–98 000, hydrolysis > 99%) of 4.69 g was first dissolved in 30 mL deionized water at 90 °C. The mixture was stirred overnight to ensure homogeneity. Then, 4.69 g AAm was added to the mixture to form a 1:1 weight ratio of PVA:AAm solution. Afterward, MBAA was added as crosslinker, TEMED as accelerator and APS as initiator in quantities of 0.0006, 0.0022, and 0.0036 times the weight of AAm, in sequence. The prepared pre-gel solution was degassed and injected into plastic molds of 70 × 50 × 1.6 mm^3, and covered by an acrylic plate. The samples were stored for 24 h for complete polymerization.

The PAAm-PVA-S hydrogel with crystalline PVA domains was synthesized after the polymerization of the PAAm-PVA hydrogel. The PAAm-PVA hydrogel was soaked in 0.6 M aqueous solution of Na_2SO_4 for 30 min. To ensure that the concentration of Na_2SO_4 in the solution keeps nearly constant before and after soaking the hydrogel, the aqueous solution was prepared with volume at least 10 times the volume of the hydrogel. After soaking, the hydrogel was taken out and stored in a sealed plastic bag for maintaining hydration. The average thickness of the samples after soaking was measured to be 1.7 mm.

Inducing anisotropy of PAAm-PVA-S hydrogels: To synthesize PAAM-PVA-S hydrogels with tunable degrees of mechanical anisotropy, a PAAm-PVA-S hydrogel was taken out immediately after its 30 min soaking in the Na_2SO_4 solution, and cut it into samples of 40 mm length and 70 mm width. The samples were then stretched and fixed to an acrylic frame with a prescribed stretch λ_{fix}. The frame and sample were stored in a sealed plastic bag for 120 h, to allow further directional crystallization of aligned PVA chains. Afterward, the samples were dismounted from the acrylic frame, and stored in the sealed bag for additional 24 h before testing (see Figure S4e, Supporting Information, for the complete processing history from synthesis to test). The degree of anisotropy was controlled by different values of λ_{fix}. The anisotropic hydrogels were cut and tested in the direction parallel to λ_{fix} (aligned) and the direction perpendicular to λ_{fix} (transverse).

Mechanical testing: All mechanical tests were conducted with the tensile machine Instron Model 5966 with a 500 N load cell. Unless otherwise specified, all the testing samples were prepared as rectangular shape of 10 mm length and 50 mm width, with thickness measured individually for different sample types (e.g., with or without Na_2SO_4 and under different λ_{fix}). The samples were adhered to two pairs of acrylic grips by Krazy glue and then mounted into the tensile machine before testing. All the samples were tested after 6 days of their storage in sealed bags, except for the daily measurement of stress–stretch curves in Figure 2a,b.

Uniaxial tensile testing: A sample of length H was mounted in the tensile machine. During the test, the sample was stretched to λH, under a constant strain rate 0.05 s^{-1}. The tensile machine recorded the force as a function of extension. The nominal stress s (i.e., the force divided by the cross-sectional area of hydrogel in the undeformed state) was calculated and plotted as a function of stretch λ. The shear modulus μ was obtained as 1/4 of the initial slope of the stress–stretch curve, under the pure shear setup.[29] As mentioned before, all the samples were 10 mm length and 50 mm width, except for the PAAm-PVA-S hydrogel samples in the transverse direction with $\lambda_{fix} = 1.1$, 1.2, and 1.3 (8 mm length and 40 mm width), since the initial sizes of the hydrogels prepared under these conditions were smaller than 50 mm. For the measurement of daily change of stress–stretch curves (Figure 2a,b), an untested sample was used in each measurement.

Fracture toughness measurement: The fracture toughness of the hydrogels was measured following the pure shear setup.[20] A sample was pre-cut by a razor blade with an initial crack of 0.4 times its width. The sample was then stretched under a strain rate of 0.05 s^{-1}. The fracture toughness Γ was calculated as $\Gamma = W(\lambda_c)H$, where $W(\lambda)$ is the integral of stress–stretch curve of the uncut sample, and λ_c is the critical

stretch when fast fracture is observed. In the test, λ_c was defined as the stretch where the stress–stretch curve of the pre-cut sample reaches the peak.

Cyclic loading tests: A sample was cut with a pre-existing flaw of 3 mm length from the middle of one side, and then stretched following a linear cyclic loading profile (Figure 4a) under a stretch amplitude λ_{max} and a strain rate of 0.5 s^{-1}. To minimize dehydration during the test, an acrylic chamber was made and it was sealed around the tensile machine. Water droplets were sprayed on the inner surface of the chamber before the test. The sample was weighed before and after each test, and found no more than 3% weight loss.

Recording the experiments: A digital camera (Cannon 70D) was used to record the loading samples in the experiments. For short-term tests (≈ minutes), videos of the complete tests were taken. For long-term tests (≈ hours), pictures of the samples were taken every 15 min. The videos and pictures were post-processed for analysis.

Preparing hydrogels for confocal microscopy: For confocal microscopy, PAAm-PVA hydrogels were prepared following the same procedure, but adjusted the PVA:AAm weight ratio to 0.5:1, for better control of linking the fluorescent dyes to PVA. Three types of hydrogels were prepared, including the PAAm-PVA hydrogel without Na_2SO_4, the unaligned PAAm-PVA-S hydrogel with Na_2SO_4, and the aligned PAAm-PVA-S hydrogel with $\lambda_{fix} = 2.5$. After 6 days of storage in sealed bags, the samples were taken out and further stained with fluorescent labeling.

Labeling hydrogel samples with fluorescence: Sodium bicarbonate ($NaHCO_3$, 792519) and sodium hydroxide (NaOH, 795429) were purchased from Sigma Aldrich. 5-(4,6-dichlorotriazinyl) aminofluorescein (5-DTAF, D16) was purchased from ThermoFisher Scientific as the fluorescent dye. The fluorescent dye 5-DTAF was linked to the hydroxide groups on PVA (see Figure S5, Supporting Information, for the corresponding chemical reaction). First, 0.1 M $NaHCO_3$ aqueous solution was prepared, with pH = 9.0 adjusted by dripping 0.1 M NaOH solution. Afterward, 5-DTAF powders were dissolved into the solution to form a 0.2 mg mL^{-1} 5-DTAF solution. Three individual containers were prepared with the same 5-DTAF solution, and incubated each type of the hydrogel sample into each individual container for 5 min at room temperature. The volume of 5-DTAF solution was made 10 times the volume of the hydrogel sample. After 5 min, the hydrogel samples were taken out and rinsed in deionized water for 2 h to remove the unreacted fluorescent dyes. The samples were then stored in sealed and fully covered tubes to avoid light in 5 °C environment for 12 h before the testing.

Confocal microscopy: A confocal microscope (Leica tcs-sp5) was used to map the domains of hydrogen bonding in the hydrogel sample. The dyes were excited with an Argon laser of 488 nm band, and images of 520 nm band were recorded.

Supporting Information

Supporting Information is available from the Wiley Online Library or from the author.

Acknowledgements

This work was supported by MRSEC (DMR-14-20570). X. P. M. was supported by the Cabeaux-Jacobs BAEF fellowship and by John A. Paulson School of Engineering and Applied Sciences at Harvard. The authors thank Professor David A. Weitz for the use of confocal microscope. The authors thank Dr. Yinan Shen for the helpful discussion on the confocal microscopy experiments.

Conflict of Interest

The authors declare no conflict of interest.

Keywords

anisotropy, fatigue, flaw-insensitivity, fracture, hydrogels

Received: December 3, 2018
Revised: January 21, 2019
Published online:

[1] C. Keplinger, J. Y. Sun, C. C. Foo, P. Rothemund, G. M. Whitesides, Z. Suo, *Science* **2013**, *341*, 984.
[2] H. Yuk, S. Lin, C. Ma, M. Takaffoli, N. X. Fang, X. Zhao, *Nat. Commun.* **2017**, *8*, 14230.
[3] J. Y. Sun, C. Keplinger, G. M. Whitesides, Z. Suo, *Adv. Mater.* **2014**, *26*, 7608.
[4] S. S. Robinson, K. W. O'Brien, H. Zhao, B. N. Peele, C. M. Larson, B. C. Mac Murray, I. M. Van Meerbeek, S. N. Dunham, R. F. Shepherd, *Extreme Mech. Lett.* **2015**, *5*, 47.
[5] D. Wirthl, R. Pichler, M. Drack, G. Kettlguber, R. Moser, R. Gerstmayr, F. Hartmann, E. Bradt, R. Kaltseis, C. M. Siket, S. E. Schausberger, S. Hild, S. Bauer, M. Kaltenbrunner, *Sci. Adv.* **2017**, *3*, e1700053.
[6] M. Qin, M. Sun, R. Bai, Y. Mao, X. Qian, D. Sikka, Y. Zhao, H. J. Qi, Z. Suo, X. He, *Adv. Mater.* **2018**, *30*, 1800468.
[7] M. Sun, R. Bai, X. Yang, J. Song, M. Qin, Z. Suo, X. He, *Adv. Mater.* **2018**, *30*, 1804916.
[8] M. Choi, M. Humar, S. Kim, S. H. Yun, *Adv. Mater.* **2015**, *27*, 4081.
[9] X. Pu, M. Liu, X. Chen, J. Sun, C. Du, Y. Zhang, J. Zhai, W. Hu, Z. L. Wang, *Sci. Adv.* **2017**, *3*, e1700015.
[10] C. Yang, Z. Suo, *Nat. Rev. Mater.* **2018**, *3*, 125.
[11] C. H. Yang, B. Chen, J. J. Lu, J. H. Yang, J. Zhou, Y. M. Chen, Z. Suo, *Extreme Mech. Lett.* **2015**, *3*, 59.
[12] C. H. Yang, B. Chen, J. Zhou, Y. M. Chen, Z. Suo, *Adv. Mater.* **2016**, *28*, 4480.
[13] C. Larson, B. Peele, S. Li, S. Robinson, M. Totaro, L. Beccai, B. Mazzolai, R. Shepherd, *Science* **2016**, *351*, 1071.
[14] C. C. Kim, H. H. Lee, K. H. Oh, J. Y. Sun, *Science* **2016**, *353*, 682.
[15] C. Chen, Z. Wang, Z. Suo, *Extreme Mech. Lett.* **2017**, *10*, 50.
[16] X. Zhao, *Proc. Natl. Acad. Sci. USA* **2017**, *114*, 8138.
[17] G. Bao, Z. Suo, *Appl. Mech. Rev.* **1992**, *45*, 355.
[18] J. P. Gong, Y. Katsuyama, T. Kurokawa, Y. Osada, *Adv. Mater.* **2003**, *15*, 1155.
[19] J. P. Gong, *Soft Matter* **2010**, *6*, 2583.
[20] J. Y. Sun, X. Zhao, W. R. Illeperuma, O. Chaudhuri, K. H. Oh, D. J. Mooney, J. J. Vlassak, Z. Suo, *Nature* **2012**, *489*, 133.
[21] M. A. Haque, T. Kurokawa, J. P. Gong, *Soft Matter* **2012**, *8*, 8008.
[22] J. Li, Z. Suo, J. J. Vlassak, *J. Mater. Chem. B* **2014**, *2*, 6708.
[23] X. Zhao, *Soft Matter* **2014**, *10*, 672.
[24] P. Lin, S. Ma, X. Wang, F. Zhou, *Adv. Mater.* **2015**, *27*, 2054.
[25] T. Zhang, S. Lin, H. Yuk, X. Zhao, *Extreme Mech. Lett.* **2015**, *4*, 1.
[26] Y. Yang, X. Wang, F. Yang, H. Shen, D. Wu, *Adv. Mater.* **2016**, *28*, 7178.
[27] Y. S. Zhang, A. Khademhosseini, *Science* **2017**, *356*, eaaf3627.
[28] R. Bai, J. Yang, Z. Suo, *Eur. J. Mech. - A/Solids* **2019**, *74*, 337.
[29] J. Tang, J. Li, J. J. Vlassak, Z. Suo, *Extreme Mech. Lett.* **2017**, *10*, 24.
[30] R. Bai, Q. Yang, J. Tang, X. P. Morelle, J. Vlassak, Z. Suo, *Extreme Mech. Lett.* **2017**, *15*, 91.
[31] R. Bai, J. Yang, X. P. Morelle, C. Yang, Z. Suo, *ACS Macro Lett.* **2018**, *7*, 312.
[32] W. Zhang, X. Liu, J. Wang, J. Tang, J. Hu, T. Lu, Z. Suo, *Eng. Fract. Mech.* **2018**, *187*, 74.
[33] W. Zhang, J. Hu, J. Tang, Z. Wang, J. Wang, T. Lu, Z. Suo, *ACS Macro Lett.* **2019**, *8*, 17.

[34] R. O. Ritchie, *Nat. Mater.* **2014**, *13*, 435.
[35] W. Yang, V. R. Sherman, B. Gludovatz, E. Schaible, P. Stewart, R. O. Ritchie, M. A. Meyers, *Nat. Commun.* **2015**, *6*, 6649.
[36] M. E. Launey, M. J. Buehler, R. O. Ritchie, *Annu. Rev. Mater. Res.* **2010**, *40*, 25.
[37] U. G. Wegst, H. Bai, E. Saiz, A. P. Tomsia, R. O. Ritchie, *Nat. Mater.* **2015**, *14*, 23.
[38] J. S. Jurvelin, M. D. Buschmann, E. B. Hunziker, *Proc. Inst. Mech. Eng., Part H* **2003**, *217*, 215.
[39] R. Ritchie, *Mater. Sci. Eng., A* **1988**, *103*, 15.
[40] J. Hutchinson, *Theor. Appl. Mech.* **1989**, 139.
[41] N. A. Peppas, P. J. Hansen, *J. Appl. Polym. Sci.* **1982**, *27*, 4787.
[42] L. E. Millon, H. Mohammadi, W. K. Wan, J. Biomed. *J. Biomed. Mater. Res., Part B* **2006**, *79B*, 305.
[43] H. Bodugoz-Senturk, C. E. Macias, J. H. Kung, O. K. Muratoglu, *Biomaterials* **2009**, *30*, 589.
[44] S. Patachia, C. Florea, C. Friedrich, Y. Thomann, *eXPRESS Polym. Lett.* **2009**, *3*, 320.
[45] M. Iwaseya, M. Watanabe, K. Yamaura, L.-X. Dai, H. Noguchi, J. Mater, *Science* **2005**, *40*, 5695.
[46] E. Otsuka, A. Suzuki, *J. Appl. Polym. Sci.* **2009**, *114*, 10.
[47] M. Véron, Y. Bréchet, F. Louchet, *Acta Mater.* **1996**, *44*, 3633.
[48] W. Lu, Z. Suo, *Phys. Rev. B* **2002**, *65*, 085401.
[49] J. W. Hutchinson, Z. Suo, *Adv. Appl. Mech.* **1991**, *29*, 63.
[50] M.-Y. He, J. W. Hutchinson, *J. Appl. Mech.* **1989**, *56*, 270.
[51] G. Lake, A. Thomas, *Proc. R. Soc. London. Series A. Math. Phys. Sci.* **1967**, *300*, 108.
[52] R. O. Ritchie, *Int. J. Fract.* **1999**, *100*, 55.
[53] P. C. Painter, M. M. Coleman, *Essentials of Polymer Science and Engineering*, DEStech Publications, Inc, Lancaster **2008**.
[54] R. Marissen, *Mater. Sci. Appl.* **2011**, *02*, 319.
[55] J.-B. Le Cam, E. Toussaint, *Macromolecules* **2010**, *43*, 4708.
[56] N. Saintier, G. Cailletaud, R. Piques, *Mater. Sci. Eng., A* **2011**, *528*, 1078.
[57] M. Yamada, S. Sugaya, Y. Naganuma, M. Seki, *Soft Matter* **2012**, *8*, 3122.
[58] S. Choi, J. Kim, *J. Mater. Chem. B* **2015**, *3*, 1479.
[59] P. Lin, T. Zhang, X. Wang, B. Yu, F. Zhou, *Small* **2016**, *12*, 4386.
[60] M. T. I. Mredha, Y. Z. Guo, T. Nonoyama, T. Nakajima, T. Kurokawa, J. P. Gong, *Adv. Mater.* **2018**, *30*, 1704937.